Modeling of Carbon-11-Acetate Kinetics by Simultaneously Fitting Data from Multiple ROIs Coupled by Common Parameters

Raymond R. Raylman, Gary D. Hutchins, Rob S. B. Beanlands and Markus Schwaiger

University of Michigan Medical Center, Department of Internal Medicine, Division of Nuclear Medicine, Ann Arbor, Michigan

One of the unique aspects of PET is its ability to noninvasively quantify metabolic processes. Metabolic rate parameters are estimated by fitting the time-activity curves from regions of interest (ROIs) placed on dynamic PET images with a kinetic model. In many cases it is possible to couple these datasets with common parameters, such as the time delay between arrival of tracer in the ROIs and the sampling site. **Methods:** Data from eight ROIs placed about images of the myocardium were coupled by the parameters describing the metabolite concentration in the blood. The method was evaluated by comparing estimates of k_2 made using the coupled region method and the standard process of fitting data from each region separately. In addition, comparisons were made between estimates of k_2 and measured myocardial oxygen consumption. **Results:** Very little change in mean values of k_2 was obtained. The variances, however, were reduced by an average of 37%, compared to the standard method, when the common parameters were not constrained. When the values of the common metabolite parameters were constrained to values previously measured, the average variance in estimates of k_2 was reduced by 30%. **Conclusion:** We have demonstrated that the use of this technique can significantly increase the precision of estimates of myocardial oxygen consumption utilizing ^{11}C-acetate PET images. More precise estimates of such quantities can facilitate detection of small regional and/or temporal physiological changes measured with PET. Furthermore, this method can be utilized whenever it is known a priori that one or more kinetic model parameters has the same value for every set of ROI data.

Key Words: PET; kinetic modeling; carbon-11-acetate

J Nucl Med 1994; 35:1286–1291

PET has demonstrated its value as a tool for quantifying physiological processes. PET studies of the brain have measured such quantities as perfusion (*1–3*), glucose metabolism (*4–6*) and receptor densities (*7–9*). Cardiac studies have investigated myocardial perfusion (*10–12*), neurophysiology (*13–15*) and metabolism (*16–18*). Quantitative PET requires the acquisition of the tissue and arterial concentration of tracer as a function of time. Blood tracer-concentration curves are obtained either by direct arterial sampling or use of image-based techniques (*19–20*). Tissue time-activity curves are acquired from a dynamic series of reconstructed PET images. Data are extracted from specifically delineated regions of interest (ROIs). The rate of physiological processes are estimated by fitting the tissue curves with a parametric model. This type of analysis can be performed for multiple ROIs and/or multiple infusions. In some cases it is known a priori that one or more of the model parameters have the same value for every set of ROI data. For example, the time delay between tracer concentration measured in the blood and that measured in the brain is common to all ROI data. Huesman and Coxson have proposed the simultaneous fitting of data from multiple ROIs coupled by common parameters (*21*). This method effectively increases the amount of information used to estimate each parameter, resulting in reduced variance. Our goal is to determine the benefits gained by applying this technique to dynamic PET measurements of myocardial oxygen consumption with ^{11}C-acetate.

The correlation between myocardial oxygen consumption and ^{11}C-acetate kinetics has been established in animal and human models (*22–28*). Typically the falling edge of the tissue time-activity curve is fit with a mono- or bi-exponential function, the resulting parameter(s) is used as a measure of oxidative metabolism. In addition, Buck et al. have demonstrated that the k_2 parameter of a two-compartment model of ^{11}C-acetate kinetics correlates well with measured myocardial oxygen consumption in a canine model (*29*). More recently, Beanlands et al. have shown the same correlation in humans (*30*). The predominant metabolic by-product of ^{11}C-acetate is ^{11}C-labeled carbon dioxide ($^{11}CO_2$), so a significant amount of this substance will be present in the blood (especially later in the study). The conventional exponential fitting analysis does not account for the presence of metabolites, and is therefore susceptible to error in estimating oxygen consumption.

Buck et al. (*29*) have corrected for the recirculating metabolites by modeling the kinetics of ^{11}C-acetate with a

Received Sept. 30, 1994; revision accepted Apr. 7, 1994.

For correspondence or reprints contact: Raymond R. Raylman, PhD, University of Michigan Medical Center, 3480 Kresge III, Box 0552, 204 Zina Pitcher Pl., Ann Arbor, MI 48109-0552.

two-compartment model, and a pair of parameters used to correct the input function for the presence of ^{11}C-acetate metabolites. The magnitude of these parameters is common to all the data obtained from ROIs drawn on the PET images. The kinetic modeling of ^{11}C-acetate in the myocardium, therefore, is well suited for examination of the coupled-ROI fitting technique. Data used in this work were obtained from a previous study measuring regional myocardial oxygen consumption (MVO_2) in patients with idiopathic dilated cardiomyopathy (*30*). Two methods of fitting the data were compared, the standard process (where data from each ROI is fit individually) and the coupled-ROI fitting method.

THEORY

Curve-fitting algorithms search parameter space for a local minimum on the χ^2 hypersurface. When multiple data sets are fit, this value can be expressed as a Taylor expansion of χ^2,

$$\chi_i^2 \approx \chi_{io}^2 + (p^i - p'^i)^T(\Phi^i)^{-1}(p^i - p'^i). \quad \text{Eq. 1}$$

In this equation, χ_{io}^2 is the minimum value of χ^2 for a fit to the i^{th} data set, p'^i is the value of the parameter vector at the minimum, and Φ is the covariance matrix of the single fit parameter estimate p'^i. The function χ^2 is a measure of how well the model simulates the data. The parameter vector p'^i can be separated into two sub-vectors: p_a^i which is different for each ROI data set and p_b which is the sub-vector containing the common parameters.

The vector p^i and matrix Φ are written as:

$$p^i = \begin{pmatrix} p_a^i \\ p_b \end{pmatrix}, \Phi^i = \begin{pmatrix} \Phi_{aa}^i & \Phi_{ab}^i \\ \Phi_{ba}^i & \Phi_{bb}^i \end{pmatrix}. \quad \text{Eq. 2}$$

The variances of the parameters estimated from the simultaneous fit are given by (*21*):

$$\Phi(p_a''^i, p_a''^i) = \Phi_{aa}^i - \Phi_{ab}^i(\Phi_{bb}^i)^{-1}\Phi_{ba}^i + \Phi_{ab}^i(\Phi_{bb}^i)^{-1}\left(\sum_{k=1}^{N}(\Phi_{bb}^k)^{-1}\right)^{-1}(\Phi_{bb}^i)^{-1}\Phi_{ba}^i, \quad \text{Eq. 3}$$

and

$$\Phi(p_b'', p_b'') = \left(\sum_{k=1}^{N}(\Phi_{bb}^k)^{-1}\right)^{-1}. \quad \text{Eq. 4}$$

The variables $p_a''^i$ are estimates of the model parameters from the simultaneous fit of the i^{th} dataset and p_b'' are the estimates of the common parameters. It is important to note that the model parameter variances are reduced by an amount governed by the strength of their coupling with the common parameters (Φ_{ab}^i).

METHODS

Carbon-11-Acetate Kinetics

The kinetics of ^{11}C-acetate in the myocardium were modeled by:

$$C_T(t_m) = (1 - BV)\int_{t_1}^{t_2} K_1 e^{-k_2 t} \otimes C_c(t)\,dt + BV\int_{t_1}^{t_2} C_a(t)\,dt. \quad \text{Eq. 5}$$

The expression $C_T(t_m)$ is the ^{11}C-acetate concentration measured at the frame midpoint (t_m). The spillover of activity from the blood pool into the myocardium due to resolution effects and vascularization is estimated using the blood volume term BV. K_1 is a model parameter which is proportional to the flow of tracer into the myocardium. The parameter k_2 is proportional to the rate at which radioactivity is transported back into the blood, it is correlated with the oxidative metabolism of ^{11}C-acetate (*29,30*). The term $C_c(t)$ is the metabolite-corrected input function and $C_a(t)$ is the measured input function. The first part of Equation 5 models the tissue concentration of tracer. Since the recirculating $^{11}CO_2$ is not absorbed by the myocardium, the input function corrected for metabolite accumulation is utilized. The second expression accounts for the contamination of the tissue curves by "spilling over" of blood pool activity into the myocardial regions due to resolution effects and vascularization. The PET tomograph is not able to distinguish between events originating from ^{11}C-acetate and $^{11}CO_2$, so both radiolabeled tracers contribute to the contamination. Thus, the uncorrected input function ($C_a(t)$) must be used to model this phenomenon. The limits of the integration t_1 and t_2 are the start and stop times of the individual frames. The symbol $\otimes$ represents the mathematical operation of convolution.

Metabolite Correction

The equation for the metabolite-corrected input function is (*29*):

$$C_c(t) = (1 - \alpha(1 - e^{-(\ln 2/\mu)t}))C_a(t). \quad \text{Eq. 6}$$

In this expression $C_c(t)$ and $C_a(t)$ have the same definition as in Equation 5. The parameters α and μ are the scale and half time of the function modeling the accumulation of $^{11}CO_2$ in blood.

ROI Placement

Eight contiguous sector-shaped ROIs were placed around the myocardium on resliced short-axis views at the mid-basal level. An attempt was made to bracket the myocardium with the inner and outer boundaries of the sectors. The size of the sectors varied from patient to patient depending upon the caliber of the left ventricle and thickness of the myocardium. Many of the resliced myocardiums were not circular, hence some sectors did not entirely encompass the target tissue. These factors may cause variation in the total number of counts contained in each of the ROI datasets.

Figure 1 schematically shows ROI labeling and placement on the myocardial image. The input function was measured by placing a small (20 square pixels) circular ROI in the center of the left ventricle at the mid-basal level. This ROI was placed in the center of the left ventricle so that signal contamination due to spillover from the myocardium was minimized. Hence, no correction for signal spillover from the myocardium into the blood pool was performed. Data from all regions were corrected for radioactive decay prior to modeling. On-line correction for patient motion was not available at the time of this study.

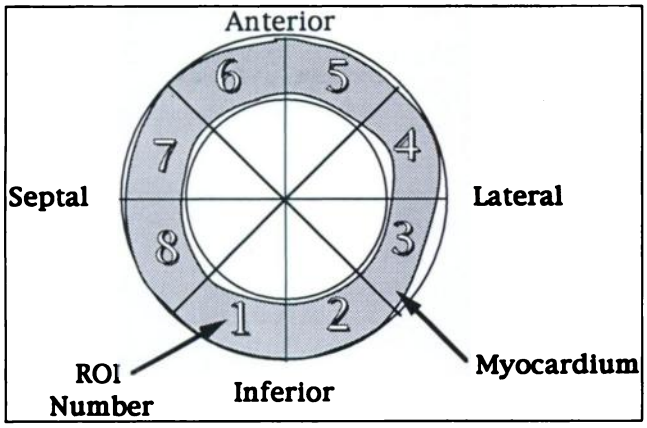

FIGURE 1. Placement of ROIs on images of the myocardium.

Fitting Procedure

The complete set of data from all eight ROIs were fit simultaneously with the model (given by Equation 5), in addition to one set of metabolite-correction parameters (α and μ), described in Equation 6. Thus, the values of the model parameters (K_1, k_2, and BV) estimated for each of the eight ROI datasets were coupled by α and μ. The effect of constraining the values of the metabolite parameters was studied by first fitting the data with no constraints (except that α was limited to values <1). These results were compared to the k_2 parameter estimates obtained with the metabolite parameters constrained to specific ranges. For α, the range extended from 0.83 to 0.93, and from 5.51 to 9.53 min for μ. These values were obtained for humans by Buck et al. (*29*). The constraints were applied as "hard edges," thus if the magnitude of a parameter exceeded the limit, it was reduced (or increased if the lower limit was crossed) by 10% and its value re-checked. If the parameter was within the acceptable range, the fitting algorithm proceeded, otherwise the parameter was again changed by 10%. This procedure continued until an acceptable magnitude was reached. For this patient population, metabolite parameters exceeded the acceptable range in approximately 25% of the trials, with the parameter α most commonly out of range. Finally, data from the eight ROIs were fit using the uncoupled method, where eight values of K1, k_2, BV, α and μ were estimated.

All fitting was performed with an unweighted nonlinear least-squares Marquardt algorithm. Values of k_2 for the eight regions were combined to produce a mean and standard deviation (s.d.). Studies have demonstrated that the oxygen consumption of the normal human heart is uniform throughout its circumference (*27*), which was verified for the data obtained from the patient population used in this work. In addition, Hutchins et al. have shown that the value of "shape parameters," such as k_2, are independent of the blood volume term BV (*31*). Hence, variations in the amount of blood pool activity included in data from each region should not affect k_2 estimates. Therefore, the s.d. calculated from the k_2 estimates for the eight regions should reflect the variation in k_2 caused by statistical noise and other sources of error not related to physiologically induced inhomogeneities.

PET Protocol

Patients were positioned in a 931 Siemens PET scanner (Hoffman Estates, IL). This scanner has eight circular rings of BGO detectors and produces 15 contiguous transaxial images with a thickness of 6.75 mm. A 20-min transmission scan was performed and the data used to correct for photon attenuation. Twenty millicuries (740 MBq) of ^{11}C-acetate were infused intravenously over 30 sec. A 30-min dynamic scan sequence was simultaneously initiated. The acquisition protocol was tailored to reduce bias and variance induced by insufficient temporal sampling (10 × 10 sec, 5 × 100 sec, 3 × 180 sec and 2 × 300 sec) (*32*). Following the baseline study, an infusion of 5 μg/kg/min of dobutamine was started. Dobutamine is a $\beta - 1$, $\beta - 2$, and $\alpha - 1$ adrenoreceptor stimulant which is used to simulate exercise stress (*33*). The infusion was increased by 5 μg/kg/min every 5 min to increase the cardiac output by 50%. Fifteen minutes after a stable infusion rate was established (mean dose = 13.2 ± 9.2 μg/kg/min), a second dose of ^{11}C-acetate was administered. The same image acquisition sequence used for the baseline study was initiated.

Myocardial Oxygen Consumption Measurement

Five patients with idiopathic dilated cardiomyopathy were selected for the study. They were included if their left-ventricular function was impaired with an ejection fraction <30% and showed no signs of ischemia. After right heart catheterization, a dual-port/triple thermistor Baim Coronary Sinus Flow Catheter (*34*) was placed in the coronary sinus. Coronary venous and radial artery samples were drawn to measure myocardial oxygen consumption. The coronary sinus catheter became dislodged in one patient and another patient was not suitable for dobutamine infusion, consequently 8 data points instead of 10 were obtained from the five patients. The study protocol was reviewed and approved by the Human Subjects Committee at the University of Michigan Medical Center on August 15, 1991 and the Radiation Safety Committee at the University of Michigan Medical Center on October 15, 1990. Informed consent was obtained from all subjects. Since the method for measuring myocardial oxygen consumption is so highly invasive, normal volunteers were not included in this study.

RESULTS

Values of k_2 (mean ± s.d.) estimated by fitting each of the eight regions separately (without constraints on the metabolite parameters) plotted as a function of measured myocardial oxygen consumption are shown in Figure 2A. Figure 2B displays similar data except that k_2 was estimated using the simultaneous fitting process. Both plots demonstrate good correlation between the parameter k_2 and MVO_2. The increase in the correlation coefficient (R) calculated for the coupled simultaneous-fit curve is not statistically different from the value calculated for the single region method ($p < 0.05$ is considered significant). The relationship between these two sets of data was examined by plotting the results for the coupled-ROI method versus k_2s estimated with the single-ROI algorithm (Fig. 3). The slope of the line fit to this function is close to unity, indicating very little change in mean values of k_2. The magnitude of variance reduction was also evaluated. The mean coefficient of variation (COV) in k_2 was reduced by 37.0% (note the reduction of the error bars in Fig. 2A) due to the utilization of the coupled-fitting procedure, these results are included in Table 1. Also shown in this table are the results of the same analysis with constraints placed on the common parameters. These data are very similar to unconstrained parameter findings. Also, the correlation coeffi-

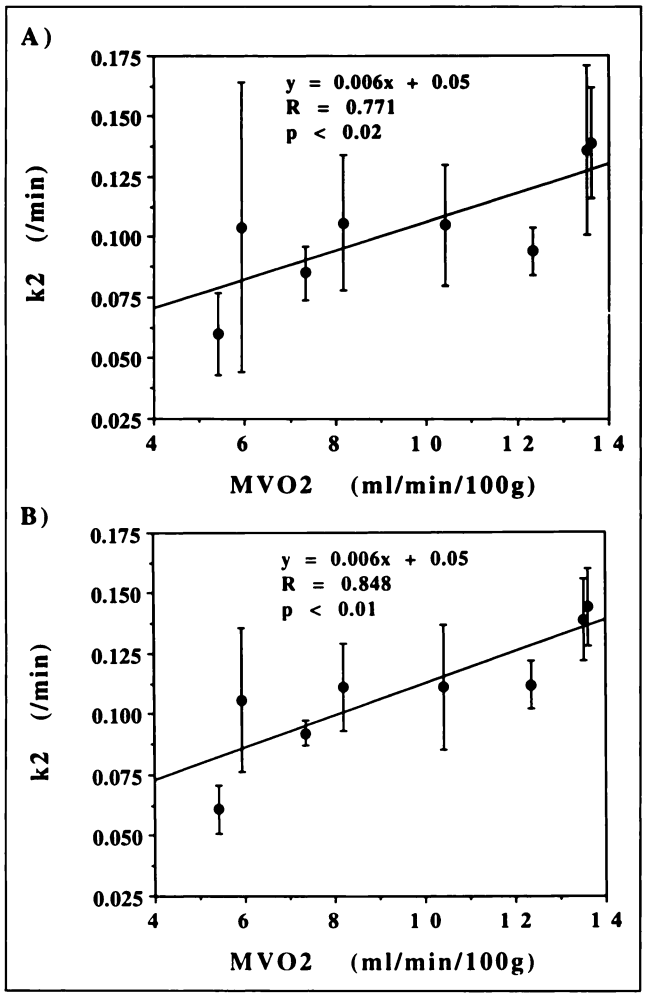

FIGURE 2. Estimates of k_2 plotted as a function of regional myocardial oxygen consumption (MVO_2) for the case where no constraints were placed on the common parameters. (A) k_2s estimated using the standard method of fitting data; (B) k_2s estimated using the coupled-ROI method.

cients for the values of k_2 plotted versus MVO_2 for each data set are presented.

DISCUSSION

The unique ability of PET to quantify metabolic processes has made it a valuable biomedical research tool. Data from ROIs drawn on a set of dynamic PET images produce time-activity curves of radiolabeled tracer in the tissue and blood. Fitting these curves with a kinetic model enables estimates of metabolic rate parameters to be calculated. Huesman and Coxson have demonstrated that when data from multiple ROIs share common parameter(s), a simultaneous fitting approach will reduce variance in the estimated parameters. To investigate the usefulness of this procedure in clinical dynamic cardiac PET studies, the estimated values of k_2 obtained from subjects with idiopathic dilated cardiomyopathy utilizing ^{11}C-acetate were correlated with measured myocardial oxygen consumption. Estimates of k_2 from the conventional method of fitting individual ROIs were compared to k_2s obtained by fitting the coupled data simultaneously. The results revealed that more precise estimates were obtained using the simultaneous fitting of data from coupled ROIs than those calculated using the standard procedure.

The plots in Figure 2 and results presented in Table 1 demonstrate that the correlation between k_2 and myocardial oxygen consumption (MVO_2) is good for this patient population. It is actually somewhat higher than that measured by Buck in canines (*29*), but slightly lower than the correlation reported between k_{mono} (the parameter in the monoexponential analysis) and MVO_2, also measured in canines by Armbrecht (*27*). Although this difference is not statistically significant, it is possible that the disease state of the subjects affected the relationship between k_2 and MVO_2. Unfortunately, the highly invasive nature of the MVO_2 measurement makes inclusion of normal subjects in this protocol prohibitive. Therefore, it is not possible to determine if the state of the subjects is responsible for the slightly reduced correlation.

Furthermore, consistency in choice of cardiac level used for data analysis was found to be a crucial factor in obtaining good correlation between k_2 and MVO_2. Previous studies have shown that myocardial oxygen consumption in normal subjects is not uniform along the short-axis of the heart. Hicks has reported that values of k_{mono} in apical slices where 8.5% lower ($p < 0.05$) than those in basal and mid-basal planes (*35*). In our patient population, we found that mean values of k_2 in the mid-basal cardiac levels were 2.9% lower ($p < 0.05$) than in basal and apical slices. Some subjects, however, exhibited differences between mid-basal and apical mean values of up to 12.2% ($p < 0.05$), which may be due to changes in myocardial oxygen resulting from the disease state of the patients. Therefore, sampling the same cardiac level throughout the datasets is critical to producing consistent results.

From the plot in Figure 3 and the correlation coefficients

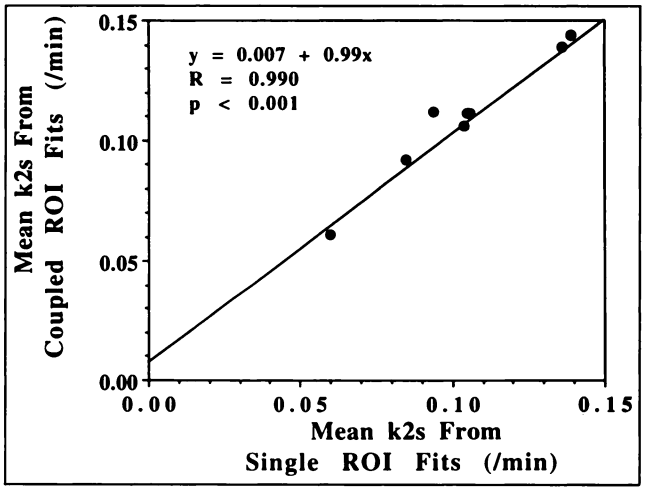

FIGURE 3. Mean values of k_2 estimated using the coupled-ROI method plotted versus the mean values of k_2 estimated with the standard method standard single ROI process.

TABLE 1
Mean Coefficient of Variation and Correlation Coefficients for Single and Coupled ROI Fitting Methods

Metabolite parameters	Fitting method	Mean		Correlation coefficient (R)
		COV (%)	ΔCOV (%)	
Unconstrained	Single regions	23.5 ± 10.6	—	0.771
Unconstrained	Coupled regions	14.8 ± 7.9	−37.0	0.848
Constrained	Single regions	22.3 ± 10.2	—	0.797
Constrained	Coupled regions	15.6 ± 8.2	−30.0	0.821

COV = coefficient of variation.

shown in Table 1, it is clear that the coupled fitting process has very little effect on the magnitude of estimates of k_2. The primary benefit of this method, therefore, is the variance reduction which is obtained for estimates of k_2. Our results demonstrate that, for this group of subjects, the mean COV in k_2 estimates was greatly reduced (37% with unconstrained common parameters and 30% with constrained parameters). This reduction results from the inclusion of more data into the parameter estimation process. Individual data points have a diminished effect on the value of each model parameter, minimizing the variance introduced in parameter estimates by "noisy" data. Increased parameter precision can facilitate the detection of small changes in metabolic rate constants (such as k_2), thereby allowing for the tracking of physiological processes over time. This ability is necessary if quantitative PET is to become effective in treatment evaluation.

Although these results demonstrate that the consolidation of common parameters into the simultaneous fitting of data from multiple ROIs reduces the effects of statistical noise in estimates of k_2, other sources of error are still present. For example, the single-ROI fit estimate of k_2 at an MVO_2 of 5.92 ml/min/100 g, shown in Figure 2A, has a large COV of 44%. Application of the coupled-ROI algorithm was only able to reduce this value to 28.3%. The major portion of the remaining error is probably caused by a large patient motion artifact detected in this dataset. Furthermore, error introduced by physical phenomena such as Compton scattering, partial volume effect and count rate limitations are also unchanged by this method and must be dealt with separately. The results obtained in this study are particular to estimates of k_2 for a two-compartment model of ^{11}C-acetate kinetics using metabolite correction parameters. The amount of error reduction must be evaluated individually for other applications. Since the amount of variance reduction is determined to a great extent by the amount of coupling between the common parameter(s) and the parameter(s) of interest (Equation 3), situations where this coupling is strong will benefit the most.

In addition to obtaining more precise parameter estimates, this method facilitates multi-ROI comparisons. Often it is necessary to compare the metabolic activity in one anatomical region to another. For example, oxygen utilization rates in different myocardial regions can be compared to assess tissue damage resulting from an ischemic event. The conventional method of fitting the data from each ROI separately will be susceptible to error induced by variance in estimates of the common parameters. The simultaneous fit method utilizes only one set of common parameters, thus eliminating this source of error and allowing for more accurate comparisons.

CONCLUSION

In this work we have demonstrated that estimates of regional myocardial oxygen consumption precision can be increased by simultaneously fitting multiple ROIs coupled by a set of metabolite parameters. The use of this method can be expanded to studies which necessitate multiple infusions and/or analysis of multiple image planes. It will be especially effective in applications where the common parameter(s) are strongly coupled to the model parameter(s) of interest. This procedure has demonstrated its usefulness in improving quantitative measurements made with PET and thus warrants further utilization.

ACKNOWLEDGMENTS

This work was supported, in part, by a training grant from the National Cancer Institute (NCI 5T32 CA 09015-17) and by a grant from the United States Department of Energy (DE GF02-87ER 60561). Dr. Beanlands was supported by a Medical Research Council of Canada Centennial Fellowship Award.

REFERENCES

1. Hoffman JM, Coleman RE. Perfusion quantification using positron emission tomography. *Invest Radiol* 1992;27(suppl. 2):s22–s26.
2. Mehdorn HM, Vyska K, Machulla HJ, Knust EJ. Use of 3-fluoro-deoxyglucose for the assessment of cerebral perfusion and glucose transport. II. Evaluation of patients undergoing EC-IC bypass surgery. *Neurol Res* 1985; 7:68–74.
3. Kuhl DE, Phelps ME, Kowell AP, et al. Effects of stroke on local cerebral metabolism and perfusion: mapping by emission computed tomography of ^{18}FDG and $^{13}NH_3$. *Ann Neurol* 1980;8:47–60.
4. Peppard RF, Martin WR, Carr GD, et al. Cerebral glucose metabolism in Parkinson's disease with and without dementia. *Arch Neurol* 1992;49:1262–1286.
5. Young AB, Penney JB, Starsota-Rubinstein S, et al. Normal caudate glucose metabolism in persons at risk for Huntington's disease. *Arch Neurol* 1987;44:254–257.
6. Mazziotta JC, Phelps ME, Miller J, Kuhl DE. Tomographic mapping of human cerebral metabolism: normal unstimulated state. *Neurology* 1981; 31:503–516.

7. Sedvall G, Farde L, Persson A, Wiesel FA. Imaging of neurotransmitter receptors in the living human brain. *Arch Gen Psychiatry* 1986;43:995–1005.
8. Wong DF, Wagner HN Jr, Dannals RF, et al. Effects of age on dopamine and serotonin receptors measured by positron emission tomography in the living human brain. *Science* 1984;226:1393–1396.
9. Delforge J, Loc'h C, Hantraye P, et al. Kinetic analysis of central [^{76}Br] bromosiluride binding to dopamine D2 receptors studied by PET. *J Cereb Blood Flow Metab* 1991;11:914–925.
10. Niemeyer MG, Kuijper AF, Gerhards LJ, D'Haene EG, van der Wall EE. Nitrogen-13-ammonia perfusion imaging: relation to metabolic imaging. *Am Heart J* 1993;125:848–854.
11. Schwaiger M, Muzik O. Assessment of myocardial perfusion by positron emission tomography. *Am J Cardiol* 1991;67:35D–43D.
12. Krivokapich J, Smith GT, Huang S-C, et al. Nitrogen-13-ammonia myocardial imaging at rest and with exercise in normal volunteers. Quantification of absolute myocardial perfusion with dynamic positron emission tomography. *Circulation* 1989;80:1328–1337.
13. Syrota A. In vivo study of receptors for neuromediators with PET. *Int J Rad Appl Instrum [B]* 1986;13:127–134.
14. Wieland DM, Rosenspire KC, Hutchins GD, et al. Neuronal mapping of the heart with 6-[^{18}F]-fluorometaraminol. *J Med Chem* 1990;33:956–964.
15. Schwaiger M, Hutchins GD, Kalff V, et al. Evidence for catecholamine uptake and storage sites in the transplanted human heart by positron emission tomography. *J Clin Invest* 1991;87:1681–1690.
16. Schelbert HR, Phelps ME, Shine KI. Imaging metabolism and biochemistry—a new look at the heart. *Am Heart J* 1983;105:522–526.
17. Camici P, Ferrannini E, Opie LH. Myocardial metabolism in ischemic heart disease: basic principles and applications to imaging by positron emission tomography. *Prog Cardiovasc Dis* 1989;32:217–238.
18. Spinks TJ, Araujo LI, Camici P. Regional myocardial glucose metabolism in angina pectoris obtained from positron emission tomography. *J Thorac Imaging* 1988;3:56–63.
19. Phelps ME, Mazziotta JC, Schelbert HR, eds. *Positron emission tomography and autoradiography*. New York: Raven Press; 1986:286–347.
20. Weinberg IN, Huang S-C, Hoffman EJ. Validation of PET acquired input functions for cardiac studies. *J Nucl Med* 1988;29:241–247.
21. Huesman RH, Coxson PG. Consolidation or common parameters in dynamic PET data analysis. *IEEE NS Conference Record* 1990:1572–1576.
22. Armbrecht JJ, Buxton DB, Schelbert HR. Validation of [1-^{11}C] acetate as a tracer for noninvasive assessment of oxidative metabolism with positron emission tomography in normal, ischemic, postischemic, and hyperimic canine myocardium. *Circulation* 1990;81:1594–1605.
23. Henes CG, Bergmann SR, Walsh MN, Sobel BE, Geltman EM. Assessment of myocardial oxidative metabolic reserve with positron emission tomography and carbon-11-acetate. *J Nucl Med* 1989;30:1489–1499.
24. Walsh MN, Geltman EM, Brown MA, et al. Noninvasive estimates of regional myocardial oxygen consumption by positron emission tomography with carbon-11-acetate in patients with myocardial infarction. *J Nucl Med* 1989;30:1798–1808.
25. Brown MA, Marshall DR, Sobel BE, Bergmann SR. Delineation of myocardial oxygen utilization with carbon-11-acetate. *Circulation* 1987;76:687–696.
26. Brown MA, Myears DW, Bergmann SR. Noninvasive assessment of canine myocardial oxygen metabolism with carbon-11-acetate and positron emission tomography. *J Am Coll Cardiol* 1988;1054–1063.
27. Armbrecht JJ, Buxton DB, Brunken RC, Phelps ME, Schelbert HR. Regional myocardial oxygen consumption determined noninvasively in humans with [1-^{11}C] acetate and dynamic positron emission tomography. *Circulation* 1989;80:863–872.
28. Krivokapich J, Huang S-C, Schelbert HR. Assessment of the effects of dobutamine on myocardial blood flow and oxidative metabolism in normal human subjects using nitrogen-13-ammonia and carbon-11-acetate. *Am J Cardiol* 1993;71:1351–1356.
29. Buck A, Wolpers HG, Hutchins GD, et al. Effect of carbon-11-acetate recirculation on estimates of myocardial oxygen consumption by PET. *J Nucl Med* 1991;32:1950–1957.
30. Beanlands RSB, Bach DS, Raylman RR, et al. The acute effects of dobutamine on myocardial oxygen consumption and cardiac efficiency measured using carbon-11-acetate kinetics in patients with dilated cardiomyopathy. *J Am Coll Cardiol* 1993;22:1389–1398.
31. Hutchins GD, Caraher JM, Raylman RR. A region of interest strategy for minimizing resolution distortions in quantitative myocardial PET studies. *J Nucl Med* 1992;33:1243–1250.
32. Raylman RR, Caraher JC, Hutchins GD. Sampling requirements for dynamic cardiac PET studies using image-derived input functions. *J Nucl Med* 1993;34:440–447.
33. Mason JR, Palac RT, Freeman ML, et al. Thallium scintigraphy during dobutamine infusion: nonexercise-dependent screening test for coronary artery disease. *Am Heart J* 1984;107:481–485.
34. Baim D, Rothman M, Harrison D. Simultaneous measurement of coronary venous blood flow and oxygen saturation during transient alterations in myocardial oxygen supply and demand. *Am J Cardiol* 1982;49:743–752.
35. Hicks RJ, Herman WH, Kalff V, et al. Quantitative evaluation of regional substrate metabolism in the human heart by positron emission tomography. *J Am Coll Cardiol* 1991;18:101–111.